ANTIOXIDANTS & REDOX SIGNALING
Volume 24, Number 2, 2016

DOI: 10.1089/ars.2015.6315

ORIGINAL RESEARCH COMMUNICATION

Hydrogen Sulfide Attenuates Inflammatory Hepcidin by Reducing IL-6 Secretion and Promoting SIRT1-Mediated STAT3 Deacetylation

Hong Xin,[1,*] Minjun Wang,[1,*] Wenbo Tang,[2] Zhuqing Shen,[1] Lei Miao,[1] Weijun Wu,[1] Chengyi Li,[1] Xiling Wang,[1] Xiaoming Xin,[1] and Yi Zhun Zhu[1,3]

Abstract

Aims: Anemia of inflammation is quite prevalent in hospitalized patients with poor prognosis. Concerns about the effectiveness and safety of iron supplementation have arisen, driving the demand for alternative therapies. Induction of hepatic hepcidin, the master hormone of iron homeostasis, causes anemia under inflammatory conditions. Previous studies indicated that hydrogen sulfide (H_2S), the third gasotransmitter and a well-known regulator of inflammation, may inhibit the secretion of inflammatory cytokines. We thus investigated the effect of H_2S on inflammatory hepcidin induction. ***Results:*** H_2S suppressed lipopolysaccharide (LPS)-induced hepcidin production and regulated iron homeostasis in mice by decreasing serum interleukin-6 (IL-6) and Janus kinase 2 (JAK2)/signal transducer and activator of transcription 3 (STAT3) activation; similar results were obtained in Huh7 cells exposed to conditioned medium from LPS-challenged THP-1 macrophages. Intriguingly, we found H_2S also attenuated hepcidin levels in Huh7 cells and mouse primary hepatocytes in a sirtuin 1 (SIRT1)-dependent manner. By promoting SIRT1 expression and stabilizing SIRT1-STAT3 interactions, H_2S ameliorated IL-6-induced STAT3 acetylation, resulting in reduced hepcidin production. Inhibition and silencing of SIRT1 diminished H_2S-mediated suppression of hepcidin, as opposed to SIRT1 activation and overexpression. Consistent results were observed *in vivo*. Furthermore, knockout of cystathionine γ-lyase (CSE), an endogenous H_2S synthase, exaggerated inflammatory hepcidin expression in mice. ***Innovation:*** For the first time, we elucidated the effects and possible mechanisms of H_2S on inflammatory hepcidin and established a novel regulatory link between SIRT1 and hepcidin. ***Conclusion:*** Our work demonstrates that H_2S attenuates inflammation-induced hepatic hepcidin *via* multipathways and suggests new treatment strategies for anemia of inflammation. *Antioxid. Redox Signal.* 24, 70–83.

Introduction

IRON IS ESSENTIAL for the normal physiological functioning of the human body. Either iron deficiency or overload may lead to diseases such as anemia or hemochromatosis (20). Hepcidin, a small peptide secreted primarily by the liver (18, 37), acts as a master hormone in regulating iron homeostasis (10, 12, 30). Through inducing the internalization and degradation of ferroportin, the principal cellular iron exporter, hepcidin suppresses dietary iron absorption from enterocytes as well as iron release by macrophages and hepatocytes, eventually lowering circulating iron levels (31).

Hepatic hepcidin is induced by multiple stimuli, including inflammatory signals caused by infection, autoimmune diseases, and cancer (12, 28). Elevated hepcidin levels in response to inflammation lead to hypoferremia or anemia of inflammation (11, 26). Lipopolysaccharide (LPS) is widely used to induce hepatic hepcidin and inflammatory anemia in experimental conditions (16, 29, 39, 45). It is currently well characterized that interleukin-6 (IL-6) plays the critical role

[1]Shanghai Key Laboratory of Bioactive Small Molecules, Department of Pharmacology, School of Pharmacy, Fudan University, Shanghai, China.
[2]Department of Oncology, School of Medicine, Fudan University, Shanghai, China.
[3]Department of Pharmacology, National University of Singapore, Singapore.
*These authors contributed equally to this work.

Innovation

Concerns have been raised regarding the efficiency and safety of conventional management of anemia of inflammation, illustrating an urgent need for alternative therapies. In the study, we demonstrated for the first time that H_2S could attenuate inflammatory hepcidin production by both reducing interleukin-6 (IL-6) secretion and promoting sirtuin 1 (SIRT1)-mediated signal transducer and activator of transcription 3 (STAT3) deacetylation. Meanwhile, we established a novel regulatory link between SIRT1 and hepcidin. These findings indicated H_2S-releasing compounds as innovative candidates for the treatment of inflammatory anemia.

in inflammatory hepcidin expression by activating signal transducer and activator of transcription 3 (STAT3) (9, 53). Binding of IL-6 to its receptor recruits Janus kinase 2 (JAK2) to phosphorylate STAT3. Furthermore, p-STAT3 dimers translocate to the nucleus, bind to the hepcidin promoter, and upregulate hepcidin gene transcription. Hepatic hepcidin fails to respond to inflammatory stimuli or promote anemia in either STAT3 liver-specific or IL-6 knockout mice (21, 42). In general, the IL-6/JAK2/STAT3 pathway is of great importance to inflammation-induced hepcidin expression.

Hydrogen sulfide (H_2S), which has long been known as a noxious gas, is the third gasotransmitter after nitric oxide (NO) and carbon monoxide (CO) (49). Biosynthesis of H_2S has been identified in a variety of mammalian tissues. In the liver, H_2S is endogenously produced by cystathionine β-synthase (CBS) and cystathionine γ-lyase (CSE) with L-cysteine as the substrate, in addition to 3-mercaptopyruvate sulfur transferase with 3-mercaptopyruvate (33, 38, 50). Previous studies revealed that H_2S plays a prominent role in inflammatory responses (22, 36). It inhibits leukocyte adherence (55) and oxidized low-density lipoprotein-induced macrophage inflammation (8). In addition, H_2S exerts anti-inflammatory effects by reducing inflammatory cytokine secretion and increasing anti-inflammatory and cytoprotective molecule levels (40, 50).

Considering the anti-inflammatory effects of H_2S, in addition to the dominant role the liver plays in hepcidin secretion and H_2S metabolism, we assessed whether H_2S could regulate hepcidin expression during inflammation. In the present study, we discovered for the first time that H_2S suppressed inflammatory hepcidin through both reducing IL-6 secretion and promoting sirtuin 1 (SIRT1)-mediated STAT3 deacetylation. Our findings elucidated the effects and potential mechanisms of H_2S on inflammation-induced hepcidin expression and might throw light on new therapeutic approaches for anemia of inflammation.

Results

H_2S attenuates LPS-induced hepcidin expression and regulates iron homeostasis in mice

To investigate our hypothesis that H_2S regulates inflammatory hepatic hepcidin, C57BL/6 and C3H mice were pretreated with sodium hydrosulfide (NaHS, i.p., 6 mg/kg/day) for 3 days, followed by LPS challenge (i.p., 0.5 mg/kg), as stated in the Materials and Methods section. C57BL/6 mice were sacrificed for mRNA, protein, and serum analysis 6 h after LPS stimulation. Tissue iron measurements and Perl's Prussian blue staining were conducted in C3H mice at 24 h. As shown in Figure 1A and B, hepatic hepcidin mRNA (*Hamp*) and serum hepcidin were evoked by LPS, which was significantly suppressed by NaHS. Moreover, immunoblot assays indicated that ferroportin, the membrane iron exporter that is degraded upon binding with hepcidin, was restored by NaHS treatment (Fig. 1C). Due to its enrichment of macrophages, the spleen has a dominant role in iron deposition during inflammation. We next analyzed serum iron levels and iron accumulation in the spleen. LPS lowered serum iron content in C57BL/6 mice by $\sim$30% after 6 h, which was improved by NaHS (Fig. 1D). As demonstrated in Figure 1E and F, iron accumulation in splenic macrophages of C3H mice was also significantly ameliorated by NaHS treatment.

As STAT3, which is activated by IL-6, is the most crucial transcription factor for hepcidin induction during inflammatory conditions, the effect of H_2S on the IL-6-mediated JAK2/STAT3 pathway was then investigated. NaHS tremendously lowered serum IL-6 levels (Fig. 1G) and hepatic *Il-6* mRNA expression induced by LPS (Supplementary Fig. S1A; Supplementary Data are available online at www.liebertpub.com/ars). Accordingly, phospho-JAK2 (p-JAK2) and phospho-STAT3 (p-STAT3) levels were significantly increased after LPS challenge, but attenuated by NaHS (Fig. 1H, Supplementary Fig. S1B, C). These results indicate that H_2S inhibits inflammatory hepcidin expression probably *via* reducing IL-6 levels and JAK2/STAT3 activation in mice.

H_2S inhibits hepcidin expression through decreasing IL-6 secretion in vitro

To evaluate the effects of H_2S *in vitro*, we used a conditioned medium (CM) model consisting of THP-1-derived macrophages and Huh7 hepatoma cells to mimic the pathophysiological conditions *in vivo*. A time course evaluation suggested 6 h as the peak point of hepcidin mRNA (*HAMP*) induction in Huh7 cells (Supplementary Fig. S2A). NaHS was first applied to THP-1-derived macrophages 1 h before LPS stimulation to produce different CMs, which was defined as the pretreatment (Fig. 2A). The dose range (50–300 μM) was chosen by reference to previous studies (46, 47). *HAMP* expression induced by LPS-CM was markedly suppressed by NaHS pretreatment in a concentration-dependent manner (Fig. 2B). Similar results were obtained with L-cysteine, the substrate for endogenous H_2S synthesis (Fig. 2C).

Due to its essential role in inflammatory hepcidin induction, the IL-6 content in CM was quantified by ELISA. NaHS significantly ameliorated IL-6 secretion evoked by LPS (Fig. 2D). Consistent results were observed with *IL6* mRNA levels in THP-1 cells, whereas NaHS elicited no significant effect in the absence of LPS (Supplementary Fig. S2B). To confirm the connection between the IL-6 reduction in CM and *HAMP* inhibition, anti-human IL-6-neutralizing antibody (αIL6, 0.05, and 0.5 μg/ml) was applied to THP-1 macrophages exposed to LPS. As illustrated in Figure 2E, *HAMP* induction by LPS-CM was suppressed and completely abolished by αIL6 at a higher concentration. In agreement with the decrease in IL-6 levels, JAK2 and STAT3 phosphorylation was inhibited by NaHS (Fig. 2F, Supplementary Fig. S2C, D) along with nuclear translocation of p-STAT3 (Fig. 2G). These results suggest that

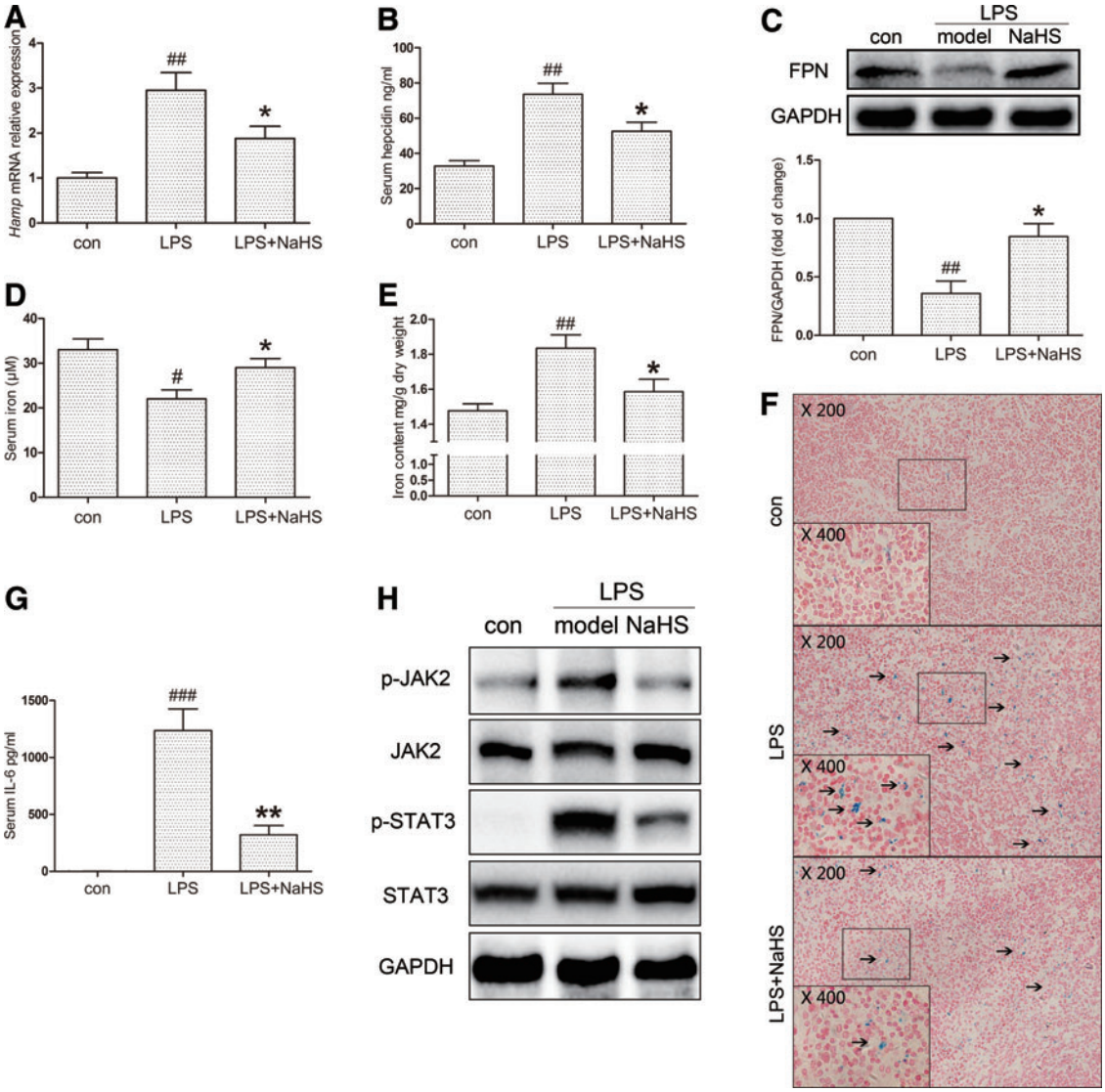

FIG. 1. H_2S suppresses LPS-induced hepcidin production and regulates iron homeostasis in mice. C57BL/6 and C3H mice were preinjected with NaHS for 3 days (i.p., 6 mg/kg/day), followed by LPS (0.5 mg/kg), as stated in the Materials and Methods section. C57BL/6 and C3H mice were killed after 6 and 24 h, respectively. **(A, B)** NaHS treatment attenuated LPS-induced hepatic *Hamp* mRNA expression **(A)** and serum hepcidin levels **(B)** in C57BL/6 mice ($n=6$). **(C)** Representative immunoblots revealed that hepatic ferroportin (FPN) protein levels in C57BL/6 mice were decreased by LPS challenge, but reversed by NaHS. Densitometry analysis is indicated below the blots ($n=6$). **(D)** Plasma iron concentrations in different groups of C57BL/6 mice ($n=6$). **(E, F)** NaHS ameliorated splenic iron accumulation induced by LPS in C3H mice 24 h after LPS challenge ($n=6$). The formation of *Prussian blue* is indicated by *solid arrows* in the representative images. **(G)** The serum IL-6 level of C57BL/6 mice was dramatically induced after LPS challenge and effectively reduced by NaHS ($n=6$). **(H)** Changes in hepatic JAK2/STAT3 activation were consistent with serum IL-6 level ($n=6$). GAPDH served as the loading control. Representative immunoblots and images are presented with densitometry analysis in the Supplementary Data. Data are presented as the mean ± SEM. $^{\#}p<0.05$, $^{\#\#}p<0.01$, and $^{\#\#\#}p<0.001$, all compared with the control group; $^{*}p<0.05$ and $^{**}p<0.01$ compared with the LPS group. GAPDH, glyceraldehyde-3-phosphate dehydrogenase; IL-6, interleukin-6; JAK2, Janus kinase 2; LPS, lipopolysaccharide; STAT3, signal transducer and activator of transcription 3. To see this illustration in color, the reader is referred to the web version of this article at www.liebertpub.com/ars

H_2S could inhibit LPS-CM-induced *HAMP* expression *via* decreasing IL-6 and JAK2/STAT3 activation.

H_2S ameliorates hepcidin expression by inhibiting STAT3 activation beyond reducing IL-6

Instead of treating macrophages with NaHS, we next applied NaHS directly to Huh7 cells exposed to the same CM, which was defined as the post-treatment here (Fig. 3A). Surprisingly, NaHS in the post-treatment model suppressed *HAMP* expression as well (Fig. 3B). Considering the critical role of IL-6 in LPS-CM, we then used recombinant human IL-6 for *HAMP* induction in Huh7 cells and similar results as observed with NaHS treatment (Fig. 3C). The effect of NaHS on IL-6-induced *HAMP* promoter activity was also evaluated by dual-luciferase reporter assay. As shown in Figure 3D,

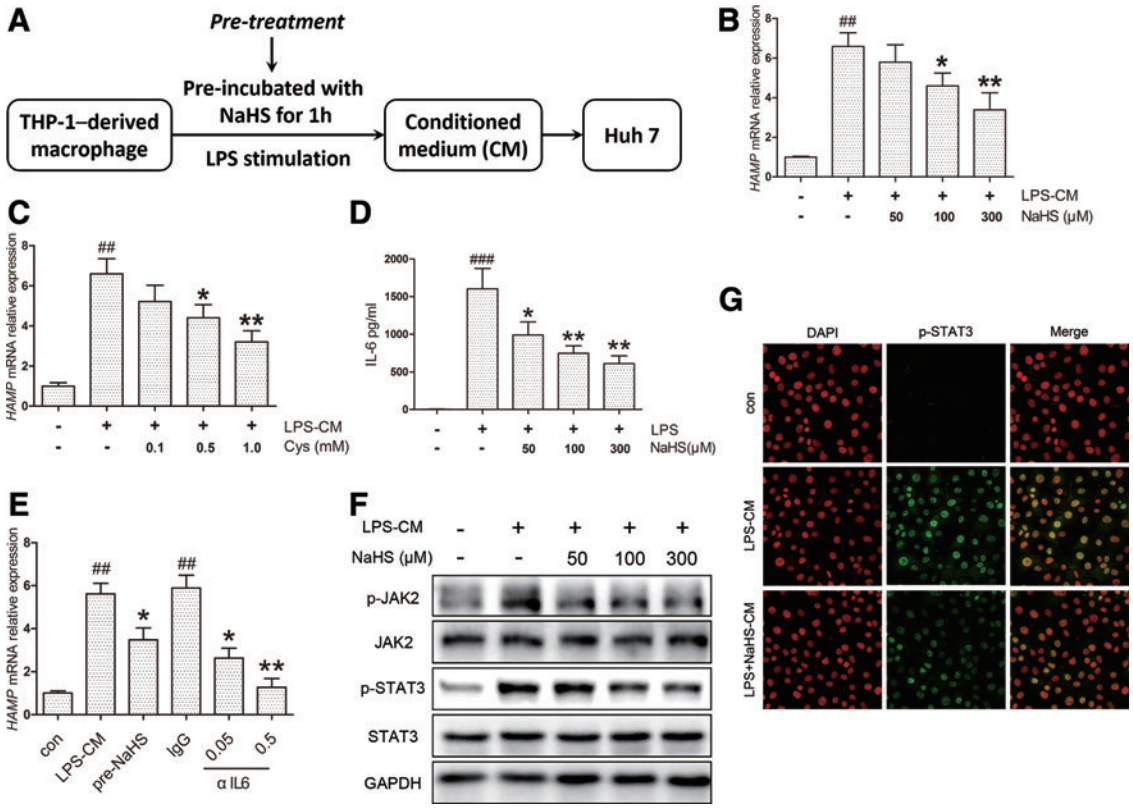

FIG. 2. H_2S inhibits hepcidin expression by decreasing IL-6 secretion in the pretreatment model *in vitro*. **(A)** A flowchart for the pretreatment in the CM model. NaHS was first applied to THP-1-derived macrophages 1 h before LPS (1 μg/ml) stimulation to produce different CMs. After 24 h, Huh7 cells were treated with these CMs for 6 h, and RNA was isolated for quantitative reverse transcription polymerase chain reaction. **(B)** NaHS suppressed *HAMP* expression in Huh7 cells induced by LPS-CM ($n=5$). **(C)** A similar effect was demonstrated with L-cysteine, the substrate for endogenous H_2S production ($n=3$). **(D)** NaHS significantly attenuated IL-6 concentration invoked by LPS in CM ($n=3$). **(E)** *HAMP* induction by LPS-CM was suppressed and completely abolished by anti-human neutralizing antibody (αIL6, 0.05, and 0.5 μg/ml) at a higher concentration ($n=3$). **(F, G)** NaHS inhibited LPS-CM-induced JAK2/STAT3 activation **(F)** and p-STAT3 translocation **(G)** in Huh7 cells. Representative immunoblots and immunofluorescence images are presented with densitometry analysis in Supplementary Data. Values are presented as mean ± SEM from at least three independent experiments. $^{\#\#}p<0.01$ and $^{\#\#\#}p<0.001$ compared with the control group; $^{*}p<0.05$ and $^{**}p<0.01$ compared with the LPS-CM or IgG group. CM, conditioned medium. To see this illustration in color, the reader is referred to the web version of this article at www.liebertpub.com/ars

NaHS decreased *HAMP* promoter activity evoked by IL-6, whereas no significant change was observed in the NaHS-only group. Moreover, NaHS ameliorated *Hamp* induction by recombinant murine IL-6 in mouse primary hepatocytes (Fig. 3E). To rule out the possibility of off-target effects, Huh7 cells were preincubated with propargylglycine (PAG) or aminooxyacetic acid (AOAA), which inhibits CSE and CBS, respectively. After preincubation with L-cysteine, the cells were challenged with IL-6 or LPS-CM. In accordance with H_2S levels in the culture medium (Supplementary Fig. S3A), inhibition of endogenous H_2S synthesis abrogated the suppression of inflammatory *HAMP* by L-cysteine (Fig. 3F), indicating the attribution of H_2S on hepcidin regulation.

In the post-treatment model, Huh7 cells were treated with either equal amounts of IL-6 or the same CM. As expected, no significant change was observed in p-JAK2 levels (Fig. 4A, Supplementary Fig. S3B). However, NaHS attenuated STAT3 phosphorylation evoked by IL-6 (Fig. 4A, Supplementary Fig. S3C), indicating that an additional pathway is involved. To further evaluate the modulation of STAT3 activation, we analyzed p-STAT3 dimerization, translocation, and transcriptional activity. As indicated in Figure 4B and C and Supplementary Figure S3D, NaHS significantly suppressed p-STAT3 dimerization induced by IL-6, accompanied by decreased nuclear translocation. The transcriptional activity of STAT3 was measured using a luciferase reporter containing five copies of the sis-inducible element (SIE) in the promoter region of the luciferase gene. IL-6 stimulation dramatically increased STAT3 transcriptional activity, which was attenuated by NaHS treatment (Fig. 4D). A similar result was demonstrated in the mRNA level of *SOCS3*, a target gene of STAT3 (Fig. 4E).

To confirm the involvement of STAT3 in *HAMP* expression, we treated Huh7 cells with stattic, a potent inhibitor of STAT3 activation. As presented in Figure 4F, stattic effectively blocked STAT3 phosphorylation induced by IL-6. As expected, *HAMP* displayed no response, and no significant change was observed with NaHS treatment (Fig. 4G).

Taken together, these results suggest that H_2S inhibits STAT3 and hepcidin activation through targeting additional pathways other than IL-6/JAK2 signaling.

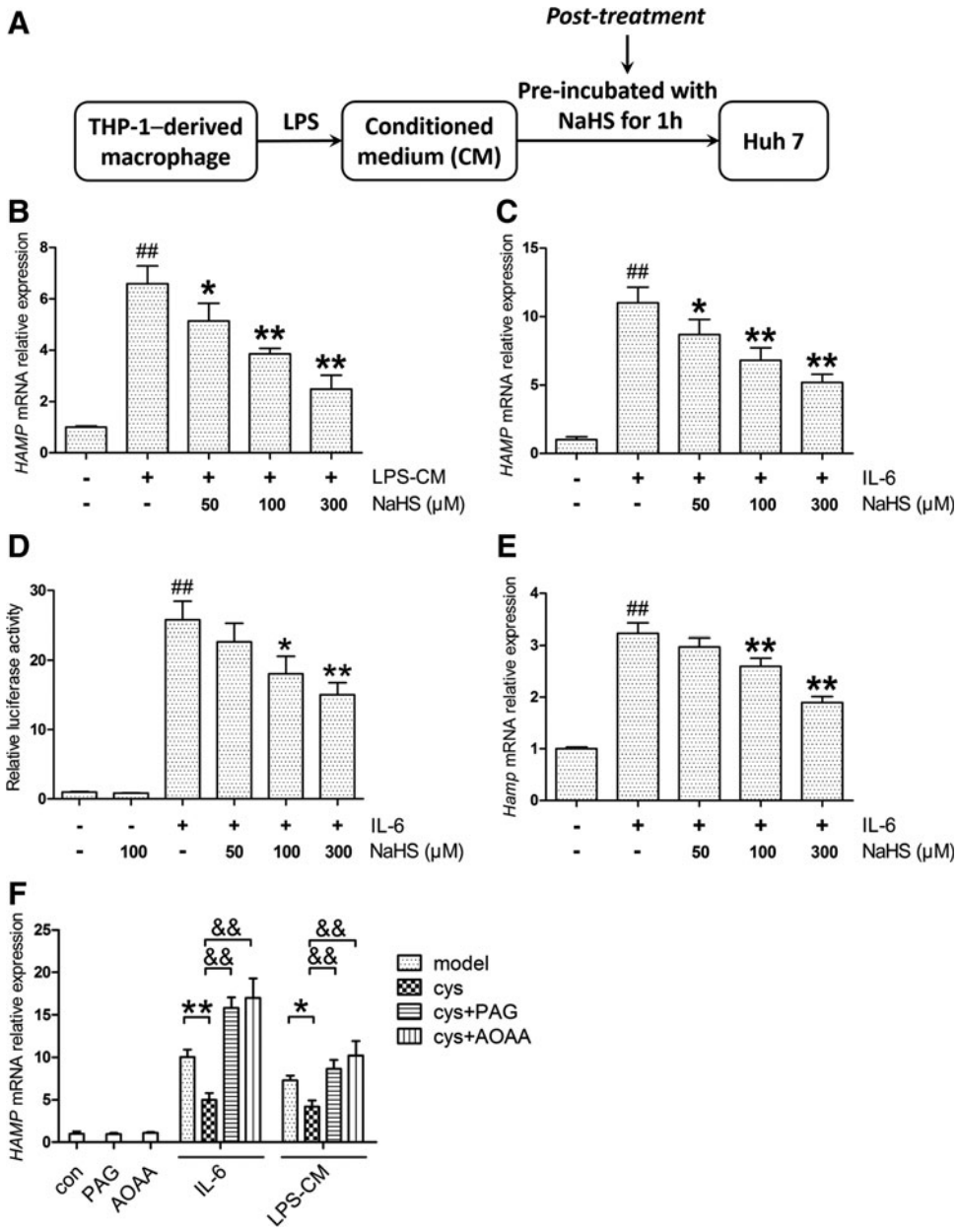

FIG. 3. H_2S ameliorates hepcidin expression and promoter activity in the post-treatment model *in vitro*. **(A)** A flowchart for the post-treatment. Huh7 cells, instead of THP-1 cells, were pretreated with NaHS for 1 h and incubated with LPS-CM for another 6 h. **(B)** NaHS suppressed *HAMP* induction in the post-treatment as well ($n=5$). **(C)** Huh7 cells were preincubated with NaHS for 1 h, and then exposed to 10 ng/ml IL-6 for 6 h. NaHS attenuated IL-6-induced *HAMP* expression in Huh7 cells ($n=5$). **(D)** NaHS decreased *HAMP* promoter activity evoked by IL-6 (10 ng/ml), but elicited no effect in the NaHS-only group ($n=3$). **(E)** Similar results were obtained in mouse primary hepatocytes stimulated with 50 ng/ml recombinant murine IL-6 ($n=5$). **(F)** Inhibition of CSE and CBS by PAG (2 m*M*) and AOAA (10 μM), respectively, abolished the L-cysteine (500 μM)-mediated suppression of *HAMP* induction by IL-6 (10 ng/ml) or LPS-CM ($n=3$). Values are presented as mean ± SEM from at least three independent experiments. $^{\#\#}p<0.01$ compared with the control group; $^{*}p<0.05$ and $^{**}p<0.01$ compared with the model group unless indicated; $^{\&\&}p<0.01$. AOAA, aminooxyacetic acid; CSE, cystathionine γ-lyase; PAG, propargylglycine.

H_2S attenuates IL-6-induced hepcidin expression through promoting SIRT1-mediated STAT3 deacetylation

Since additional mechanisms appeared to be involved in the post-treatment model, we turned our attention to factors regulating STAT3 activation. It was reported that inhibition of STAT3 acetylation (ac-STAT3) impairs its phosphorylation and transcriptional function (54). Thus, ac-STAT3 was investigated in the post-treatment model. As indicated in Figure 5A, NaHS ameliorated the ac-STAT3 levels induced by IL-6. To confirm the regulatory role of ac-STAT3 in self-phosphorylation and *HAMP* induction, we treated cells with sodium butyrate (NaBu), a histone deacetylase (HDAC) inhibitor, which raised ac-STAT3 levels in previous studies (43). NaBu markedly increased STAT3 acetylation in Huh7 cells, in parallel with the induction of p-STAT3 and *HAMP* expression, which could be abolished by stattic (Fig. 5B, Supplementary Fig. S4A). These results suggest that STAT3 acetylation regulates *HAMP* expression through self-phosphorylation.

STAT3 acetylation is precisely regulated by histone acetyltransferases and HDACs, including SIRT1 as a class III HDAC (32). Thus, we sought to access the role of SIRT1 in the post-treatment model. As expected, NaHS increased SIRT1 protein levels in Huh7 cells (Fig. 5A) and mouse primary hepatocytes (Supplementary Fig. S4B). Next, we performed coimmunoprecipitation (co-IP) to examine the effect of H_2S on the physical interaction between exogenous SIRT1 and STAT3. As shown in Figure 5C, IL-6 stimulation promoted dissociation of the SIRT1-STAT3 complex, which could be effectively stabilized by NaHS.

Then, we used EX-527, a highly selective SIRT1 inhibitor, to block SIRT1 activity. EX-527 abolished the H_2S-mediated suppression of *HAMP* expression (Fig. 5D) in accordance with the STAT3 transcriptional function assessed by SIE reporter (Supplementary Fig. S4C). Immunoblot analysis

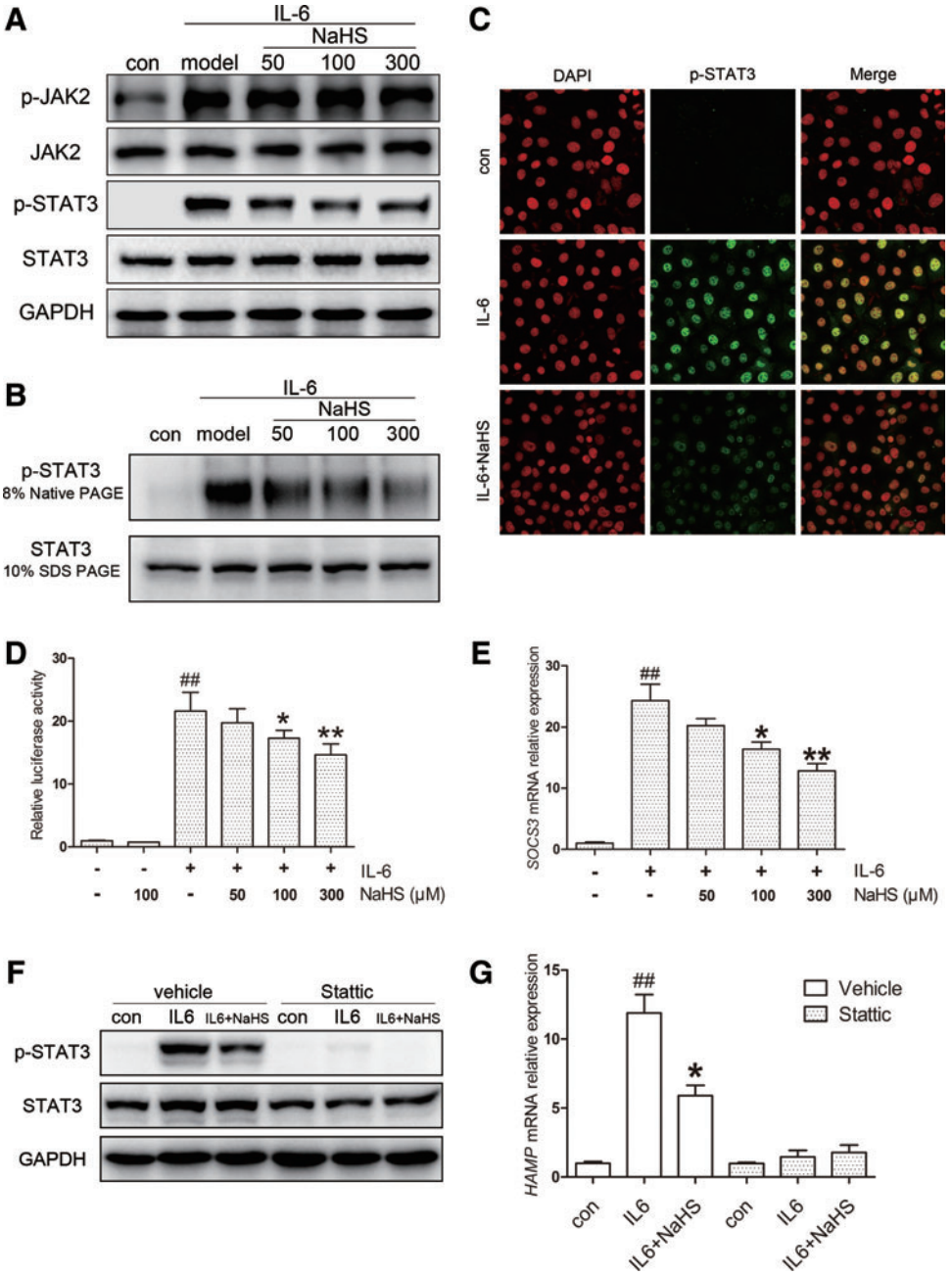

FIG. 4. H_2S attenuates IL-6-induced STAT3 phosphorylation, dimerization, translocation, and transcriptional function in a JAK2-independent manner. (A) NaHS suppressed IL-6 (10 ng/ml)-induced STAT3 phosphorylation in Huh7 cells, whereas p-JAK2 levels remained unchanged. **(B)** Representative native PAGE revealed reduced STAT3 dimerization in response to NaHS. **(C)** Representative immunofluorescence images illustrated that NaHS successfully suppressed p-STAT3 nuclear translocation induced by IL-6. **(D)** NaHS effectively inhibited IL-6 (10 ng/ml)-evoked STAT3 transcriptional activity assessed by an SIE reporter ($n = 5$). **(E)** A similar result was demonstrated for the mRNA level of *SOCS3*, a target gene of STAT3 ($n = 3$). **(F, G)** Stattic (10 μM), a potent inhibitor of STAT3 activation, dramatically blocked STAT3 phosphorylation **(F)** and *HAMP* induction **(G)** by IL-6 (10 ng/ml, $n = 3$). GAPDH served as the loading control. Representative immunoblots and immunofluorescence images are presented with densitometry analysis in the Supplementary Data. Values are presented as mean ± SEM from at least three independent experiments. $^{\#\#}p < 0.01$ compared with the control group; $^{*}p < 0.05$ and $^{**}p < 0.01$ compared with the IL-6 group. SIE, sis-inducible element. To see this illustration in color, the reader is referred to the web version of this article at www.liebertpub.com/ars

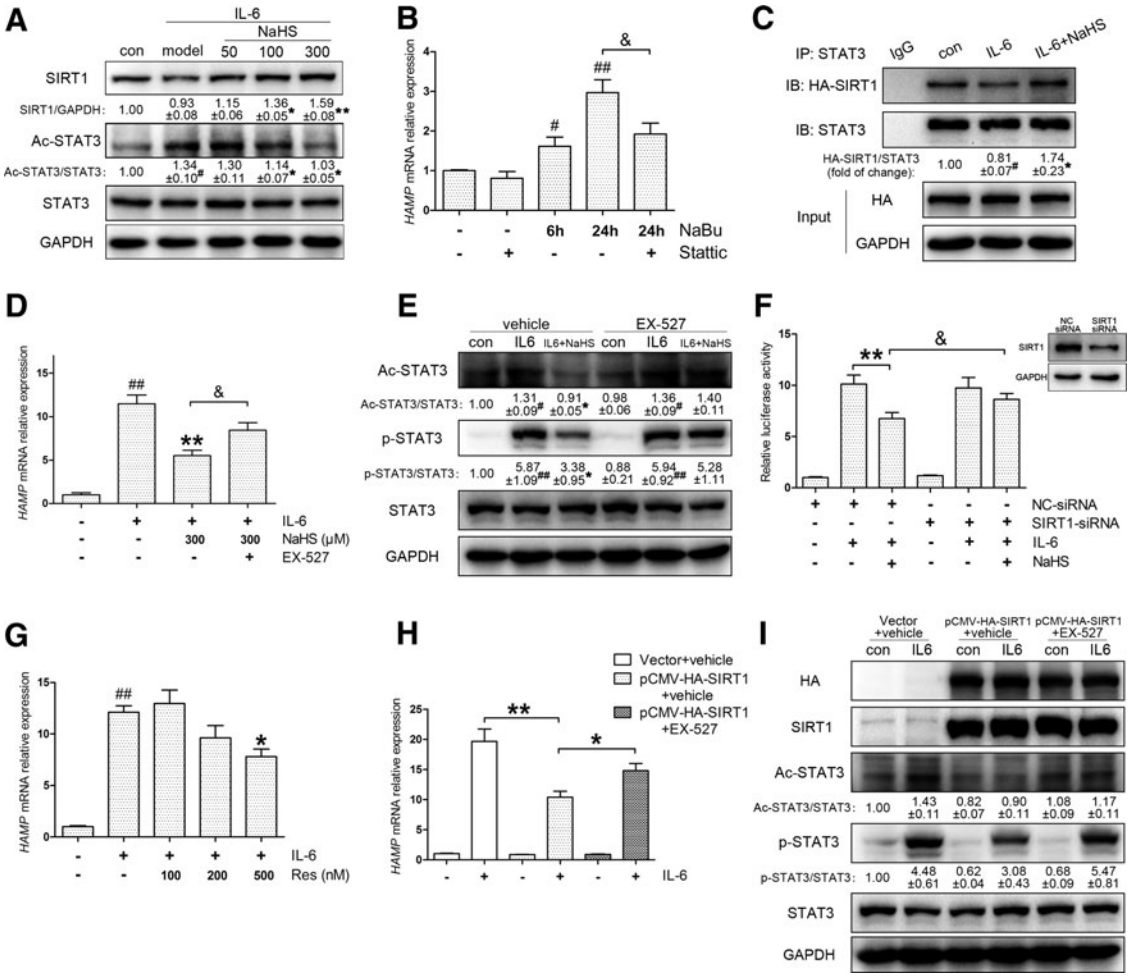

FIG. 5. H_2S suppresses IL-6-induced hepcidin expression by promoting SIRT1-mediated STAT3 deacetylation. **(A)** NaHS treatment promoted SIRT1 expression and reduced STAT3 acetylation in the presence of IL-6 in Huh7 cells. **(B)** NaBu (1 m*M*), an HDAC inhibitor that promotes STAT3 acetylation, successfully induced *HAMP* expression without IL-6. The induction was blocked by stattic (10 μM, $n=5$). **(C)** IL-6 (10 ng/ml) challenge led to the dissociation of the exogenous SIRT1-STAT3 complex, which was stabilized by NaHS in Huh7 cells. **(D, E)** EX-527 (10 μM), a potent SIRT1 inhibitor, reversed the inhibition of NaHS on *HAMP* as well as STAT3 acetylation and phosphorylation ($n=5$). **(F)** SIRT1 silencing by specific siRNA abrogated the effect of NaHS on *HAMP* promoter activity ($n=3$). Silencing efficiency is indicated in the *top right corner*. **(G)** Resveratrol, an SIRT1 activator, attenuated IL-6 (10 ng/ml)-induced *HAMP* expression ($n=3$). **(H)** SIRT1 overexpression significantly suppressed *HAMP* induction by IL-6 (10 ng/ml), which was reversed by EX-527 (10 μM) in Huh7 cells ($n=5$). **(I)** The inhibitory effects of overexpressed SIRT1 on STAT3 acetylation and phosphorylation were diminished by EX-527 (10 μM). GAPDH served as the loading control. Representative immunoblots are presented with the results of densitometry analysis. Values are presented as mean ± SEM from at least three independent experiments. $^{\#}p<0.05$ and $^{\#\#}p<0.01$ compared with the control group; $^{*}p<0.05$ and $^{**}p<0.01$ compared with the IL-6 group unless indicated; $^{\&}p<0.05$. HDAC, histone deacetylase; SIRT1, sirtuin 1.

indicated that EX-527 reversed the inhibition of STAT3 acetylation and phosphorylation by H_2S (Fig. 5E). The involvement of SIRT1 was further confirmed by gene silencing. By transient transfection of SIRT1-specific or control siRNA, *HAMP* promoter activity was evaluated, and a coincident result is presented in Figure 5F.

Afterward, the effects of SIRT1 activation and overexpression were examined. Previous studies suggest that resveratrol improves physiological function by activating SIRT1 (19); hence, we introduced resveratrol as an SIRT1 activator. As was observed with NaHS, preincubation with resveratrol ameliorated *HAMP* induction (Fig. 5G) and STAT3 activation (Supplementary Fig. S4D). Moreover, SIRT1 overexpression suppressed IL-6-evoked *HAMP* expression as well as p-STAT3 and ac-STAT3 levels, which could be abrogated by EX-527 (Fig. 5H–I). Altogether, we conclude that H_2S inhibits IL-6-evoked STAT3 activation and hepcidin expression by promoting SIRT1-mediated STAT3 deacetylation.

The effect of H_2S on inflammatory hepcidin is diminished by SIRT1 inhibition and CSE knockout in vivo

We next investigated whether the regulation of SIRT1 and ac-STAT3 could be confirmed *in vivo*. C57BL/6 mice were pretreated with either resveratrol (10 mg/kg) only or EX-527 (10 mg/kg), followed by NaHS (6 mg/kg), before LPS

(0.5 mg/kg) stimulation. As demonstrated in Figure 6A, EX-527 partially abolished the effect of NaHS. Moreover, resveratrol also inhibited hepatic *Hamp* expression. Corresponding results were also observed for serum iron content and IL-6 levels, in addition to hepatic SIRT1 and STAT3 activation (Fig. 6B–D). To better understand the H_2S-SIRT1-hepcidin interaction *in vivo*, we also examined mice injected with recombinant murine IL-6. As manifested in Supplementary Figure S5, NaHS application improved hepatic hepcidin mRNA and serum iron levels, which were reversed by EX-527. The involvement of SIRT1 was further supported by immunoblots of STAT3 activation. These results demonstrate that H_2S promotes SIRT1-mediated STAT3 deacetylation *in vivo*.

Furthermore, our hypothesis was also tested in CSE knockout ($CSE^{-/-}$) C57BL/6 mice. As one of the endogenous H_2S synthases, CSE is critical for H_2S homeostasis. Previous research by our group and other groups demonstrated that plasma H_2S levels in $CSE^{-/-}$ mice decreased by ~50% compared with those in wild-type (WT) mice (17, 44). Thus, we compared the hepatic *Hamp* response between WT and $CSE^{-/-}$ mice. As manifested in Figure 6E, no significant

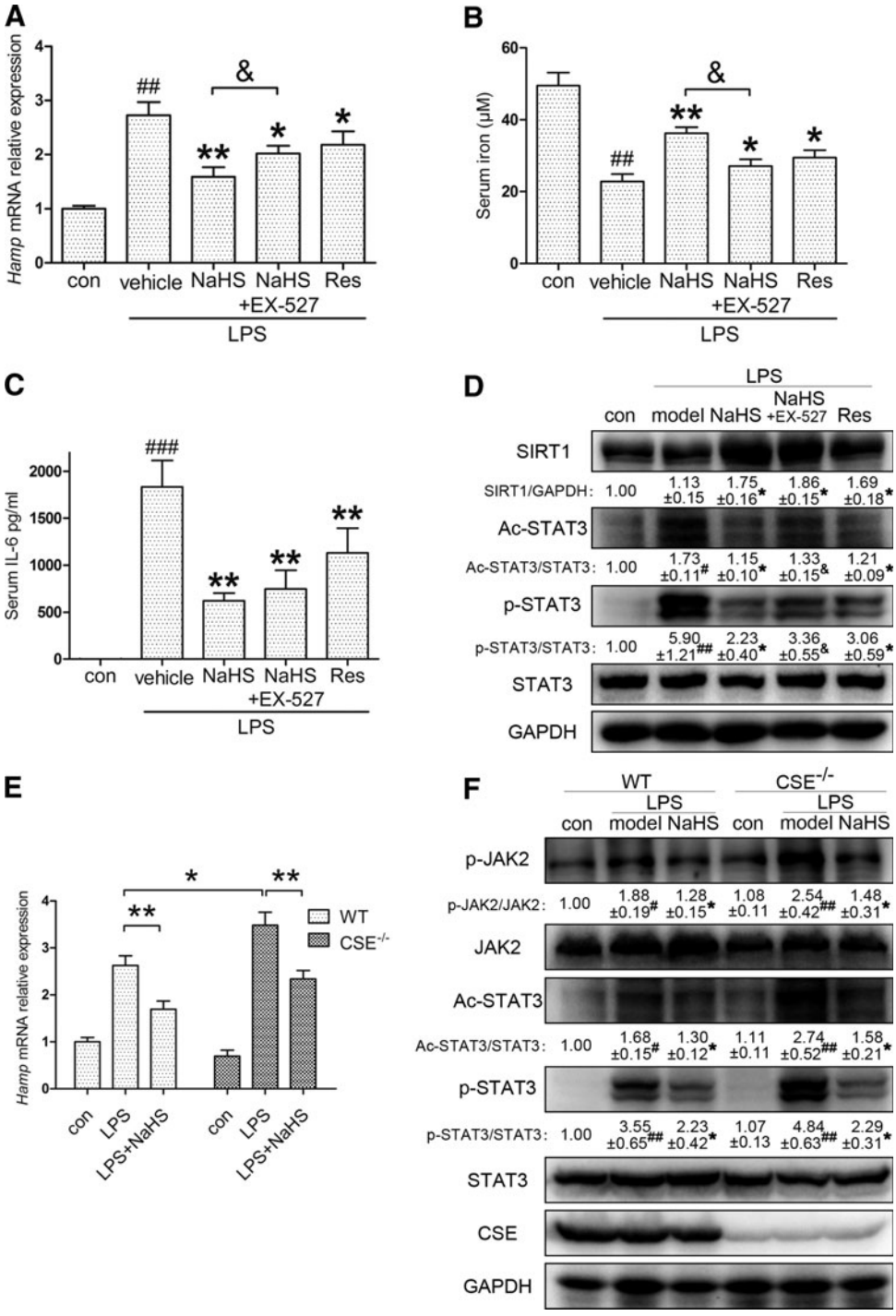

FIG. 6. Suppressive effect of H_2S on inflammatory hepcidin is diminished by SIRT1 inhibition and CSE knockout *in vivo*. **(A)** EX-527 (10 mg/kg) partially abrogated the attenuation of LPS (0.5 mg/kg)-induced *Hamp* expression by NaHS (6 mg/kg) in C57BL/6 mice. Resveratrol (10 mg/kg) also suppressed inflammatory *Hamp* induction ($n=8$). **(B–D)** Consistent results were demonstrated with serum iron and IL-6, as well as hepatic SIRT1, ac-STAT3, and p-STAT3 ($n=8$). **(E)** No significant change was observed in basal hepcidin levels after knocking out CSE. Compared with WT, CSE knockout ($CSE^{-/-}$) mice were more susceptible to LPS challenge (0.5 mg/kg), whereas NaHS (6 mg/kg) successfully reversed the intense *Hamp* induction in the liver ($n=6$–8). **(F)** Representative immunoblots indicated that CSE deficiency exacerbated LPS-induced JAK2/STAT3 activation, which was rescued by NaHS ($n=6$–8). GAPDH served as the loading control. Representative immunoblots are presented with the results of densitometry analysis. Data are presented as the mean ± SEM of three individual experiments. $^{\#}p<0.05$, $^{\#\#}p<0.01$, and $^{\#\#\#}p<0.001$ compared with the control group; $^{*}p<0.05$ and $^{**}p<0.01$ compared with the LPS group unless indicated; $^{\&}p<0.05$. WT, wild-type.

change was observed in the two control groups. However, $CSE^{-/-}$ mice were more susceptible to LPS (0.5 mg/kg) challenge, indicating the significance of endogenous H_2S homeostasis for inflammatory hepcidin production. Moreover, the intense *Hamp* induction was successfully reversed by NaHS (6 mg/kg) application. Immunoblot analysis confirmed that CSE deficiency exacerbated the LPS-induced JAK2/STAT3 activation, which was ameliorated by NaHS (Fig. 6F). These results provide strong evidence that H_2S is critical for hepcidin induction and JAK2/STAT3 activation during inflammation.

Discussion

In the present study, we discovered that H_2S suppressed inflammation-induced hepatic hepcidin production both *in vivo* and *in vitro*. H_2S significantly decreased IL-6 secretion and JAK2/STAT3 activation, which was the dominant pathway for hepcidin induction. In addition, H_2S attenuated hepcidin in Huh7 cells and mouse primary hepatocytes in an SIRT1-dependent manner. By promoting SIRT1 expression and stabilizing SIRT1-STAT3 interactions, H_2S ameliorated STAT3 acetylation irritated by IL-6. Reduced acetylation suppressed STAT3 phosphorylation and transcriptional function, as well as hepcidin induction. Inhibition or silencing of SIRT1 diminished H_2S suppression of hepcidin, whereas SIRT1 activation and overexpression blocked hepcidin induction. Consistent results were obtained *in vivo*. Furthermore, knockout of CSE, one of the endogenous H_2S synthases, exaggerated inflammatory hepcidin expression in mice. Taken together, our results bring forward SIRT1 as a new modulator of hepcidin and H_2S as a novel potential therapeutic modality for inflammatory anemia. The schematic diagram is summarized in Figure 7.

Hepcidin, initially named for its antimicrobial property, is induced during infection or inflammation. This response is regarded as a host defense mechanism against microbial proliferation, which relies on serum iron. Previous studies confirmed that IL-6, secreted from monocytes and macrophages, is responsible for inflammatory hepcidin induction through activating STAT3 (29, 41). The CM model is well accepted in relevant studies, as opposed to exposing hepatocytes to LPS directly (9). In fact, Huh7 cells and mouse primary hepatocytes barely responded to direct LPS challenge with respect to the p-STAT3 level and hepcidin expression (unpublished observations). As a result, we adopted LPS-mediated CM and recombinant IL-6 for hepcidin induction *in vitro*.

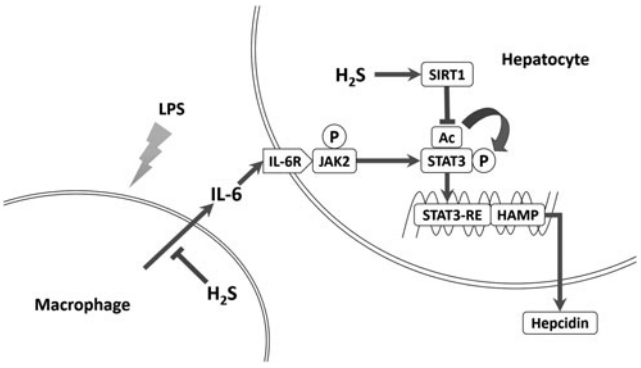

FIG. 7. Illustrative diagram of the involved pathways. H_2S attenuated inflammatory hepcidin production through two novel pathways, namely reducing IL-6 secretion *via* its anti-inflammatory property and promoting SIRT1-mediated STAT3 deacetylation, which in turn suppresses STAT3 and hepcidin activation.

As the third gasotransmitter, H_2S plays a paramount role in the regulation of signal transduction. Mounting evidence from independent groups illustrates that H_2S is tightly involved in the pathophysiological progression of diseases, such as sepsis, heart failure, and atherosclerosis (50). Since its initial discovery, however, there have been controversies over the role of H_2S in inflammation and inflammatory diseases. Currently, it appears that H_2S can have both pro- and anti-inflammatory activities depending on the dose and sampling time (14). In this work, we observed that H_2S elicited anti-inflammatory effects and suppressed IL-6 secretion in both THP-1-derived macrophages and mice, leading to decreased JAK2/STAT3 activation and hepcidin expression. Previous research indicated that H_2S inhibits NF-κB activation under inflammatory conditions, which is the most crucial pathway in the induction of proinflammatory cytokines (34, 48, 52). Thus, the suppression of NF-κB activation by H_2S is a potential mechanism involved in IL-6 suppression.

In pharmacological studies, NaHS is widely accepted as an exogenous H_2S donor. Due to its chemical property, NaHS releases H_2S in a robust manner, but for a relatively short duration after dissolution. Previous work by Whiteman *et al.* suggested that H_2S is completely released from NaHS in 1–2 h (52). To guarantee accuracy and repeatability, NaHS was freshly dissolved immediately before use. In addition, H_2S in the CM of the pretreatment model escapes completely after 24 h of incubation and thus has no overlap with that in the post-treatment model.

STAT3 is a member of the STAT family with important roles in cellular transformation, proliferation, inflammation, and metastasis of cancer (1, 6). It is well established that phosphorylation on Tyr^{705} of STAT3 is essential for its activation upon stimulation with the IL-6 superfamily. On the contrary, increasing studies indicate that STAT3 is also acetylated on some lysine residues. Yuan *et al.* first reported that STAT3 acetylation on Lys^{685} by p300 regulates its dimerization and DNA binding ability (54). Recently, Dasgupta *et al.* suggested that the integrity of Lys^{685} is required for most unphosphorylated STAT3-dependent genes (7). Furthermore, Nie *et al.* found that mutations of four key lysines of STAT3 impair its ability of phosphorylation and transactivation functions (32).

Consistently, our results suggest that the deacetylation promoted by H_2S suppresses STAT3 phosphorylation and transcriptional function under IL-6 stimulation. In addition, for the first time, we established a link between STAT3 acetylation and hepcidin expression, indicating an alternative approach for hepcidin modulation. However, the specific mechanism by which STAT3 acetylation regulates self-phosphorylation remains unclear. This regulation may be attributed to the change in STAT3 conformational transformation following acetylation since Lys^{685} locates to the end of the β-sheet region of the SH2 domain (3). It is also noteworthy that acetylation may compete with and negatively regulate protein ubiquitination and stabilization in some circumstances (23, 25).

In line with our observations, other groups have also reported STAT3 acetylation by IL-6 (35), although the mechanisms involved remain unclear. In this work, we found that IL-6 promoted the dissociation of the STAT3-SIRT1 complex. As a deacetylase, SIRT1 plays an important role in STAT3 modification. Thus, dissociation of the complex perhaps accounts for the STAT3 acetylation induced by IL-6. In support of this notion, we observed that stabilization of the STAT3-SIRT1 complex by NaHS reduced STAT3 acetylation levels, which could be abolished by the SIRT1 inhibitor, EX-527. Moreover, consistent results were also demonstrated upon exposure to the SIRT1 activator, resveratrol, as well as after SIRT1 overexpression. It is worth noting that acetylation of STAT3 is also regulated by histone acetyltransferases such as the CREB-binding protein/p300 family (51). Therefore, we conclude that the induction of STAT3 acetylation by IL-6 is, at least partially, attributable to the dissociation of the STAT3-SIRT1 interactions.

SIRT1, a mammalian ortholog of Sir2, is an NAD^+-dependent deacetylase involved in a variety of physiological process. While this article was in preparation, other independent groups also reported SIRT1 activation by H_2S (24, 56). The mechanisms in H_2S-induced SIRT1 activation remain unidentified, but increasing evidence suggests the involvement of energetic status. Concerning the STAT3-SIRT1 interaction, previous studies on hepatic gluconeogenesis have revealed that the inhibitory effect of STAT3 is regulated by the nutritional status through SIRT1-mediated deacetylation (32). In diabetic db/db mice, deletion of SIRT1 increases STAT3 acetylation and exacerbates symptoms of diabetic nephropathy (13).

Unlike basal STAT3 phosphorylation, however, the regulation of SIRT1 on IL-6-induced robust STAT3 activation and downstream hepcidin induction remains unknown. In this work, we present strong evidence that SIRT1 promotion by H_2S decreases STAT3 activation and hepcidin expression during inflammation. After all, SIRT1 plays a key role in metabolic regulation and adaptation (4, 5). Recent studies demonstrated the relationship between innate immunity and energy metabolism through antagonistic cross talk between NF-κB and SIRT1 signaling pathways (15), and hepcidin is sensed by innate immune and infectious stimuli (2). Additionally, an RNAi screen study identified that some nutrient metabolism genes might regulate hepcidin expression and iron homeostasis (27). Thus, these results suggested that SIRT1 might be a critical energy sensor connecting cellular metabolism and hepcidin expression. Further confirmatory work is necessary.

In summary, we demonstrated for the first time that H_2S suppressed inflammatory hepatic hepcidin by reducing IL-6-induced JAK2/STAT3 activation and promoting SIRT1-mediated STAT3 deacetylation. Our work provides novel insights into SIRT1-regulated hepcidin expression and clarifies the anti-inflammatory property of H_2S. Furthermore, these findings highlight H_2S-releasing compounds as innovative candidates for the treatment of inflammatory anemia.

Materials and Methods

Reagents

Sodium hydrosulfide (NaHS), L-cysteine, phorbol myristate acetate (PMA), LPS, PAG, AOAA, EX-527, resveratrol (Res), and sodium butyrate (NaBu) were purchased from Sigma-Aldrich. Stattic was purchased from Selleck Chemicals.

Recombinant human and murine IL-6, goat anti-human IL-6 antibody, and goat normal IgG were obtained from Peprotech. Antibodies to total and phospho-JAK2, total and phospho-STAT3 (Tyr^{705}), acetyl-STAT3 (Lys^{685}), and HA were purchased from Cell Signaling Technology. Antibodies to SIRT1 and glyceraldehyde-3-phosphate dehydrogenase (GAPDH) were acquired from Bioworld Technology. In addition, antibodies to ferroportin and CSE were obtained from Santa Cruz Biotechnology.

Animals

All animal care and experimental protocols complied with the Animal Management Rules of the Ministry of Health of the People's Republic of China and were approved by the Animal Care Committee of Fudan University.

Eight-week-old male C57BL/6 and C3H mice were purchased from the Sippr-bk Experimental Animal Center. The CSE knockout C57BL/6 mice were a kind gift from Shanghai Research Center of Model Organisms, Shanghai, China. Mice were housed under specific pathogen-free conditions at 25°C and maintained under a 12-h light/12-h dark cycle with *ad libitum* access to food and water. NaHS was freshly dissolved in sterilized saline and administrated intraperitoneally (i.p., 6 mg/kg/day) to mice for 3 days before LPS challenge. Saline was used as a vehicle control. On the fourth day, mice were i.p. injected with 0.5 mg/kg LPS 2 h after the last NaHS treatment. In experiments with EX-527 and resveratrol, these two reagents were dissolved in 0.5% DMSO and 0.5% Tween 20 (vol/vol) saline solution and i.p. administrated 2 h before NaHS or LPS treatment, both at 10 mg/kg. The same solvent was used as a vehicle control. C57BL/6 mice were sacrificed by cervical dislocation for mRNA, protein, and serum analysis 6 h after LPS stimulation. Tissue iron measurements and Perl's Prussian blue staining were performed in C3H mice at 24 h. All efforts were made to ameliorate animal sufferings during the experiments.

Cell culture

Cell cultures were maintained at 37°C under humidified air with 5% CO_2. Human Huh7 hepatoma cells (JCRB, Japanese Collection of Research Bioresources) were cultured in high-glucose Dulbecco's modified Eagle's medium (DMEM) supplemented with 10% fetal bovine serum (FBS; ExCell Bio) and 1% penicillin and streptomycin (Gibco). THP-1, a human monocytic cell line from ATCC, was maintained in RPMI 1640 medium with 10% FBS and 1% penicillin and streptomycin. THP-1 cells were seeded into six-well plates at 6×10^6 cells per well and treated with 100 n*M* PMA overnight to induce the differentiation into macrophage-like cells. After washing with phosphate-buffered saline (PBS), differentiated THP-1 macrophages were cultured in fresh medium for 1 day, followed by 1 μg/ml LPS stimulation for another 24 h. After centrifugation, the cell-free supernatant of the culture medium was collected as CM. Huh7 cells (5×10^5) were exposed to undiluted CM for 6 h, and then harvested for mRNA or protein analysis. For IL-6 treatment, Huh7 cells were directly incubated with 10 ng/ml recombinant human IL-6 without THP-1-derived CM.

Compound treatments

To investigate the effect of H_2S on macrophages and hepatocytes separately, NaHS was applied at two different stages—either to THP-1 or Huh7 cells—in the CM model. In one condition, the compound was applied to THP-1 cells 1 h before LPS challenge to generate different CMs, which was defined as the pretreatment in this article; in the other condition, the compound was applied to Huh7 cells 1 h before exposing to the same CM, which was defined as the post-treatment. L-cysteine, a substrate for CSE and CBS, was applied in the same manner. These two compounds were applied to Huh7 cells directly in the IL-6 stimulation model. In the enzymatic inhibition assay, cells were preincubated with the CSE inhibitor, PAG (2 m*M*), or the CBS inhibitor, AOAA (10 μM), 1 h before L-cysteine was applied.

Resveratrol, EX-527, and stattic were prepared as DMSO solutions. When cells were challenged with these compounds, the same volume of DMSO was added in parallel as a vehicle control.

Isolation and culture of mouse primary hepatocytes

Mouse primary hepatocytes were isolated from 8-week-old C57BL/6 mice using a modified two-step collagenase perfusion protocol. In brief, after anesthesia, the liver was perfused with calcium and magnesium-free Hank's balanced salt solution containing 0.5 m*M* EDTA and 0.05 *M* HEPES, followed by DMEM containing 5 m*M* calcium chloride and 0.05% type IV collagenase. The liver was then removed and isolated cells were purified with 40% Percoll (GE Healthcare Bio-Sciences). Hepatocytes were seeded onto six-well plates at a density of 8×10^5 cells per well. After 3 h, the culture medium was changed, and the cells were exposed to 50 ng/ml recombinant murine IL-6 for 6 h on the following day.

RNA isolation and real-time quantitative reverse transcription polymerase chain reaction

Total RNA from cultured cells and mouse livers was extracted with RNAiso Plus (TAKARA Bio) according to the manufacturer's instructions. Reverse transcription of total RNA was conducted with PrimeScript™ RT Master Mix (Perfect Real Time; TAKARA Bio). Primer sequences are provided in Table 1. Real-time quantitative polymerase chain reaction (PCR) was performed and semiquantified on a Bio-Rad IQ5 Real-Time PCR System with SYBR Green Premix Ex Taq (TAKARA Bio).

Plasmid and siRNA transfection

pCMV-HA vector, pCMV-HA-hSIRT1, and pCMV-FLAG-hSTAT3 were purchased from Bioworld. Plasmids were purified using a QIAprep Spin Miniprep Kit (QIAGEN). Huh7 cells were transiently transfected with 2 μg of plasmid per well for six-well plates, using Lipofectamine 2000 (Invitrogen), according to the manufacturer's instructions. Six hours later, the cells were exposed to fresh medium and cultured for another 48 h until IL-6 treatment.

For silencing experiments, Huh7 cells in 12-well plates were transfected with 100 n*M* negative control siRNA or specific siRNA against human SIRT1 (Sigma-Aldrich) using Lipofectamine 2000. The medium was replaced at 6 h post-transfection, and silencing efficiency was determined by Western blotting 72 h after transfection.

Dual-luciferase reporter assay

The human hepcidin promoter (−1000/ +71) was constructed by PCR amplification and inserted into the pGL3 basic vector (Promega Biotech) using *Mlu*I and *Xho*I restriction enzyme sites (Obio Tech). The pGL4.47 [luc2P/SIE/Hygro] vector was purchased from Promega Biotech as an SIE reporter. Huh7 cells were cotransfected with 240 ng of hHAMP-luc or SIE constructs and 8 ng of CMV Renilla control plasmid using Lipofectamine 2000. At 48 h after transfection, cells were stimulated with IL-6 for 6 h. For gene silencing experiments, Huh7 cells were cotransfected with reporter plasmids together with SIRT1-specific or control siRNA. Relative luciferase activities were determined using the Dual-Luciferase System (Promega Biotech), according to the manufacturer's instructions. All transfection experiments were performed in quadruplicate.

Immunoprecipitation and immunoblot analysis

For immunoprecipitation (IP), cells were lysed in IP-specific buffer (20 m*M* Tris–HCl, 150 m*M* NaCl, 1% Triton X-100, pH 7.5) and incubated with antibody and Protein A/G Plus-Agarose according to the manufacturer's instructions (Santa Cruz Biotechnology). Normal IgG (Santa Cruz Biotechnology) was used as a negative control. Finally, immunoprecipitates were washed four times before boiling with 2 × loading buffer.

For SDS-PAGE, livers were homogenized in RIPA lysis buffer (50 m*M* Tris–HCl, 150 m*M* NaCl, 5 m*M* EDTA, 1% Triton X-100, 1% sodium deoxycholate, and 0.1% SDS, pH 7.4) containing a protease and phosphatase inhibitor cocktail (Sigma-Aldrich). Cell samples were lysed in 1 × NuPAGE® LDS Sample Buffer (Invitrogen). Fifty micrograms of protein was subjected to SDS-PAGE gels for each sample.

For native PAGE of p-STAT3 dimers, native protein extracts were prepared in the same lysis buffer used for IP. After 30 min of lysis, cell extracts were centrifuged at

Table 1. Primer Sequences Used in Quantitative Reverse Transcription Polymerase Chain Reaction

Gene	*Forward*	*Reverse*
Hamp (M)	AGAGCTGCAGCCTTTGCAC	GAAGATGCAGATGGGGAAGT
Il-6 (M)	TGTGCAATGGCAATTCTGAT	CCAGAGGAAATTTTCAATAGGC
Actin (M)	TGTTACCAACTGGGACGACA	GGTGTTGAAGGTCTCAAA
HAMP (H)	CTGCAACCCCAGGACAGAG	GGAATAAATAAGGAAGGGAGGGG
SOCS3 (H)	CCTGCGCCTCAAGACCTTC	GTCACTGCGCTCCAGTAGAA
ACTIN (H)	AGGATGCAGAAGGAGATCACTG	GGGTGTAACGCAACTAAGTCATAG

12,000 × *g* for 10 min, and the supernatant was loaded onto 8% SDS-free PAGE gels.

After electrophoresis, protein samples were transferred to PVDF membranes (Millipore), followed by blocking with 5% skim milk and incubation with primary antibodies overnight at 4°C. The blots were then developed with horseradish peroxidase-conjugated antibodies at room temperature. Immunoreactive proteins were visualized using ECL (Millipore) and quantified by densitometry using a Bio-Rad Image Laboratory system. GAPDH served as the loading control.

Immunofluorescence staining

Huh7 cells were fixed with 4% formaldehyde and treated with ice-cold methanol for 10 min at −20°C. After blocking in PBS with 5% BSA and 0.3% Triton X-100 for 1 h at room temperature, the cells were incubated with phospho-STAT3 (Tyr^{705}) rabbit mAb diluted in PBS with 1% BSA and 0.3% Triton X-100 at 4°C overnight. Alexa Fluor 488-conjugated goat anti-rabbit IgG (Invitrogen) was used as the secondary antibody and was diluted in PBS with 0.1% Tween 20 and incubated for 1 h in the dark, followed by staining with DAPI for another 10 min. The slides were observed by confocal laser scanning microscopy (Zeiss LSM 710).

Quantification of H_2S concentration

H_2S determination was performed using the methylene blue method as described previously (44).

Serum iron, hepcidin, and IL-6 analysis

Mouse blood samples were collected in nonheparinized tubes and centrifuged at 3000 rpm for 10 min to separate serum. Serum iron content was measured using a commercial kit according to protocols described by Roche Diagnostics.

Murine serum hepcidin and IL-6, together with human IL-6 in CM, were quantified by ELISA following protocols described by the manufacturers (hepcidin kit from Uscn, IL-6 kit from Boatman).

Tissue nonheme iron analysis

Mouse spleen samples were first dried at 65°C for 48 h, and then digested in acid solution (3 *M* hydrochloric acid and 10% trichloroacetic acid) at 65°C for 24 h after weighing. Afterward, the acid extracts were centrifuged, and the supernatant was collected. 1, 10-Phenanthroline monohydrate, a heterocyclic compound widely used for photometric determination of Fe (II), was mixed with the extract at a volume ratio of 3:1 and incubated for 20 min at room temperature. The absorbance at 510 nm was measured using a spectrophotometer. A serial dilution of 45 m*M* ferrous ammonium sulfate (Sigma-Aldrich) was used to construct a calibration curve.

Perl's Prussian blue staining of paraffin-embedded sections

To evaluate iron deposition in mouse spleens, tissues were fixed in 4% formalin PBS solution, embedded in paraffin wax, sectioned, and stained with Perl's Prussian blue solution for 30 min at room temperature. A neutral red counterstain was then applied to provide a contrasting background. Images were captured using the Zeiss Axio Scope A1 system.

Statistical analysis

Data are expressed as the mean ± SEM. Statistical analysis was performed using one-way ANOVA, followed by Student's *t*-tests. Values of $p < 0.05$ were considered statistically significant.

Acknowledgments

This work was supported by grants from the National Major Scientific and Technological Special Project (No. 2012ZX09501001-001-003; 2012ZX09103101-064), National Natural Science Foundation of China (No. 81330080; 81173054), Shanghai Committee of Science and Technology of China (No. 14JC1401100), a key laboratory program of the Education Commission of Shanghai Municipality (No. ZDSYS14005), and the college students' innovation project of Fudan University (Wangdao, No.13024).

Authorship Contributions

The authors who participated in the research design were H.X. and M.W. M.W., H.X., W.T., Z.S., L.M., W.W., C.L., and X.X. conducted experiments. H.X, M.W., and X.W. performed the data analysis, and M.W., H.X., and Y.Z.Z wrote or contributed to the writing of the manuscript.

Author Disclosure Statement

No competing financial interests exist.

References

1. Aggarwal BB, Kunnumakkara AB, Harikumar KB, Gupta SR, Tharakan ST, Koca C, Dey S, and Sung B. Signal transducer and activator of transcription-3, inflammation, and cancer. *Ann N Y Acad Sci* 1171: 59–76, 2009.
2. Armitage AE, Eddowes LA, Gileadi U, Cole S, Spottiswoode N, Selvakumar TA, Ho L-P, Townsend AR, and Drakesmith H. Hepcidin regulation by innate immune and infectious stimuli. *Blood* 118: 4129–4139, 2011.
3. Becker S, Groner B, and Müller CW. Three-dimensional structure of the Stat3β homodimer bound to DNA. *Nature* 394: 145–151, 1998.
4. Blander G and Guarente L. The Sir2 family of protein deacetylases. *Annu Rev Biochem* 73: 417–435, 2004.
5. Boutant M and Cantó C. SIRT1 metabolic actions: integrating recent advances from mouse models. *Mol Metab* 3: 5–18, 2014.
6. Darnell JE. Transcription factors as targets for cancer therapy. *Nat Rev Cancer* 2: 740–749, 2002.
7. Dasgupta M, Unal H, Willard B, Yang J, Karnik SS, and Stark GR. Critical role for lysine 685 in gene expression mediated by transcription factor unphosphorylated STAT3. *J Biol Chem* 289: 30763–30771, 2014.
8. Du J, Huang Y, Yan H, Zhang Q, Zhao M, Zhu M, Liu J, Chen SX, Bu D, and Tang C. Hydrogen sulfide suppresses oxidized low-density lipoprotein (ox-LDL)-stimulated monocyte chemoattractant protein 1 generation from macrophages via the nuclear factor κB (NF-κB) pathway. *J Biol Chem* 289: 9741–9753, 2014.
9. Falzacappa MVV, Spasic MV, Kessler R, Stolte J, Hentze MW, and Muckenthaler MU. STAT3 mediates hepatic hepcidin expression and its inflammatory stimulation. *Blood* 109: 353–358, 2007.

10. Ganz T. Hepcidin in iron metabolism. *Curr Opin Hematol* 11: 251–254, 2004.
11. Ganz T. Hepcidin and iron regulation, 10 years later. *Blood* 117: 4425–4433, 2011.
12. Ganz T and Nemeth E. Hepcidin and iron homeostasis. *Biochim Biophys Acta* 1823: 1434–1443, 2012.
13. Gao R, Chen J, Hu Y, Li Z, Wang S, Shetty S, and Fu J. Sirt1 deletion leads to enhanced inflammation and aggravates endotoxin-induced acute kidney injury. *PLoS One* 9: e98909, 2014.
14. Hegde A and Bhatia M. Hydrogen sulfide in inflammation: friend or foe? *Inflamm Allergy Drug Targets* 10: 118–122, 2011.
15. Kauppinen A, Suuronen T, Ojala J, Kaarniranta K, and Salminen A. Antagonistic crosstalk between NF-κB and SIRT1 in the regulation of inflammation and metabolic disorders. *Cell Signal* 25: 1939–1948, 2013.
16. Kemna E, Pickkers P, Nemeth E, van der Hoeven H, and Swinkels D. Time-course analysis of hepcidin, serum iron, and plasma cytokine levels in humans injected with LPS. *Blood* 106: 1864–1866, 2005.
17. King AL, Polhemus DJ, Bhushan S, Otsuka H, Kondo K, Nicholson CK, Bradley JM, Islam KN, Calvert JW, and Tao Y-X. Hydrogen sulfide cytoprotective signaling is endothelial nitric oxide synthase-nitric oxide dependent. *Proc Natl Acad Sci U S A* 111: 3182–3187, 2014.
18. Krause A, Neitz S, Mägert H-J, Schulz A, Forssmann W-G, Schulz-Knappe P, and Adermann K. LEAP-1, a novel highly disulfide-bonded human peptide, exhibits antimicrobial activity. *FEBS Lett* 480: 147–150, 2000.
19. Lagouge M, Argmann C, Gerhart-Hines Z, Meziane H, Lerin C, Daussin F, Messadeq N, Milne J, Lambert P, and Elliott P. Resveratrol improves mitochondrial function and protects against metabolic disease by activating SIRT1 and PGC-1α. *Cell* 127: 1109–1122, 2006.
20. Lawen A and Lane DJ. Mammalian iron homeostasis in health and disease: uptake, storage, transport, and molecular mechanisms of action. *Antioxid Redox Signal* 18: 2473–2507, 2013.
21. Lee P, Peng H, Gelbart T, and Beutler E. The IL-6-and lipopolysaccharide-induced transcription of hepcidin in HFE-, transferrin receptor 2-, and β2-microglobulin-deficient hepatocytes. *Proc Natl Acad Sci U S A* 101: 9263–9265, 2004.
22. Li L, Bhatia M, Zhu YZ, Zhu YC, Ramnath RD, Wang ZJ, Anuar FBM, Whiteman M, Salto-Tellez M, and Moore PK. Hydrogen sulfide is a novel mediator of lipopolysaccharide-induced inflammation in the mouse. *FASEB J* 19: 1196–1198, 2005.
23. Li M, Luo J, Brooks CL, and Gu W. Acetylation of p53 inhibits its ubiquitination by Mdm2. *J Biol Chem* 277: 50607–50611, 2002.
24. Li X, Zhang K-Y, Zhang P, Chen L-X, Wang L, Xie M, Wang C-Y, and Tang X-Q. Hydrogen sulfide inhibits formaldehyde-induced endoplasmic reticulum stress in PC12 cells by upregulation of SIRT-1. *PLoS One* 9: e89856, 2014.
25. Lin R, Tao R, Gao X, Li T, Zhou X, Guan K-L, Xiong Y, and Lei Q-Y. Acetylation stabilizes ATP-citrate lyase to promote lipid biosynthesis and tumor growth. *Mol Cell* 51: 506–518, 2013.
26. Maliken BD, Nelson JE, and Kowdley KV. The hepcidin circuits act: balancing iron and inflammation. *Hepatology* 53: 1764–1766, 2011.
27. Mleczko-Sanecka K, Roche F, da Silva AR, Call D, D'Alessio F, Ragab A, Lapinski PE, Ummanni R, Korf U, and Oakes C. Unbiased RNAi screen for hepcidin regulators links hepcidin suppression to proliferative Ras/RAF and nutrient-dependent mTOR signaling. *Blood* 123: 1574–1585, 2014.
28. Nairz M, Haschka D, Demetz E, and Weiss G. Iron at the interface of immunity and infection. *Front Pharmacol* 5: 152, 2014.
29. Nemeth E, Rivera S, Gabayan V, Keller C, Taudorf S, Pedersen BK, and Ganz T. IL-6 mediates hypoferremia of inflammation by inducing the synthesis of the iron regulatory hormone hepcidin. *J Clin Investig* 113: 1271–1276, 2004.
30. Nemeth E, Roetto A, Garozzo G, Ganz T, and Camaschella C. Hepcidin is decreased in TFR2 hemochromatosis. *Blood* 105: 1803–1806, 2005.
31. Nemeth E, Tuttle MS, Powelson J, Vaughn MB, Donovan A, Ward DM, Ganz T, and Kaplan J. Hepcidin regulates cellular iron efflux by binding to ferroportin and inducing its internalization. *Science* 306: 2090–2093, 2004.
32. Nie Y, Erion DM, Yuan Z, Dietrich M, Shulman GI, Horvath TL, and Gao Q. STAT3 inhibition of gluconeogenesis is downregulated by SirT1. *Nat Cell Biol* 11: 492–500, 2009.
33. Norris EJ, Culberson CR, Narasimhan S, and Clemens MG. The liver as a central regulator of hydrogen sulfide. *Shock* 36: 242, 2011.
34. Oh G-S, Pae H-O, Lee B-S, Kim B-N, Kim J-M, Kim H-R, Jeon SB, Jeon WK, Chae H-J, and Chung H-T. Hydrogen sulfide inhibits nitric oxide production and nuclear factor-κB via heme oxygenase-1 expression in RAW264. 7 macrophages stimulated with lipopolysaccharide. *Free Radic Biol Med* 41: 106–119, 2006.
35. Ohbayashi N, Ikeda O, Taira N, Yamamoto Y, Muromoto R, Sekine Y, Sugiyama K, Honjoh T, and Matsuda T. LIF- and IL-6-induced acetylation of STAT3 at Lys-685 through PI3K/Akt activation. *Biol Pharm Bull* 30: 1860–1864, 2007.
36. Pan LL, Liu XH, Zheng HM, Yang HB, Gong QH, and Zhu YZ. S-propargyl-cysteine, a novel hydrogen sulfide-modulated agent, attenuated tumor necrosis factor-α-induced inflammatory signaling and dysfunction in endothelial cells. *Int J Cardiol* 155: 327–332, 2012.
37. Park CH, Valore EV, Waring AJ, and Ganz T. Hepcidin, a urinary antimicrobial peptide synthesized in the liver. *J Biol Chem* 276: 7806–7810, 2001.
38. Paul BD and Snyder SH. H2S signalling through protein sulfhydration and beyond. *Nat Rev Mol Cell Biol* 13: 499–507, 2012.
39. Pigeon C, Ilyin G, Courselaud B, Leroyer P, Turlin B, Brissot P, and Loréal O. A new mouse liver-specific gene, encoding a protein homologous to human antimicrobial peptide hepcidin, is overexpressed during iron overload. *J Biol Chem* 276: 7811–7819, 2001.
40. Rivers JR, Badiei A, and Bhatia M. Hydrogen sulfide as a therapeutic target for inflammation. *Expert Opin Ther Targets* 16: 439–449, 2012.
41. Rodriguez R, Jung C-L, Gabayan V, Deng JC, Ganz T, Nemeth E, and Bulut Y. Hepcidin induction by pathogens and pathogen-derived molecules is strongly dependent on interleukin-6. *Infect Immun* 82: 745–752, 2014.
42. Sakamori R, Takehara T, Tatsumi T, Shigekawa M, Hikita H, Hiramatsu N, Kanto T, and Hayashi N. STAT3 signaling within hepatocytes is required for anemia of inflammation in vivo. *J Gastroenterol* 45: 244–248, 2010.

43. Sethi G, Chatterjee S, Rajendran P, Li F, Shanmugam MK, Wong KF, Kumar AP, Senapati P, Behera AK, and Hui KM. Inhibition of STAT3 dimerization and acetylation by garcinol suppresses the growth of human hepatocellular carcinoma in vitro and in vivo. *Mol Cancer* 13: 66, 2014.
44. Shen Y, Shen Z, Miao L, Xin X, Lin S, Zhu Y, Guo W, and Zhu YZ. miRNA-30 family inhibition protects against cardiac ischemic injury by regulating cystathionine-γ-lyase expression. *Antioxid Redox Signal* 22: 224–240, 2014.
45. Shin D-Y, Chung J, Joe Y, Pae H-O, Chang KC, Cho GJ, Ryter SW, and Chung H-T. Pretreatment with CO-releasing molecules suppresses hepcidin expression during inflammation and endoplasmic reticulum stress through inhibition of the STAT3 and CREBH pathways. *Blood* 119: 2523–2532, 2012.
46. Spiller F, Orrico MI, Nascimento DC, Czaikoski PG, Souto FO, Alves-Filho JC, Freitas A, Carlos D, Montenegro MF, and Neto AF. Hydrogen sulfide improves neutrophil migration and survival in sepsis via K+ ATP channel activation. *Am J Respir Crit Care Med* 182: 360–368, 2010.
47. Suzuki K, Olah G, Modis K, Coletta C, Kulp G, Gerö D, Szoleczky P, Chang T, Zhou Z, and Wu L. Hydrogen sulfide replacement therapy protects the vascular endothelium in hyperglycemia by preserving mitochondrial function. *Proc Natl Acad Sci U S A* 108: 13829–13834, 2011.
48. Wallace JL. Hydrogen sulfide-releasing anti-inflammatory drugs. *Trends Pharmacol Sci* 28: 501–505, 2007.
49. Wang R. Hydrogen sulfide: the third gasotransmitter in biology and medicine. *Antioxid Redox Signal* 12: 1061–1064, 2010.
50. Wang R. Physiological implications of hydrogen sulfide: a whiff exploration that blossomed. *Physiol Rev* 92: 791–896, 2012.
51. Wang R, Cherukuri P, and Luo J. Activation of Stat3 sequence-specific DNA binding and transcription by p300/CREB-binding protein-mediated acetylation. *J Biol Chem* 280: 11528–11534, 2005.
52. Whiteman M, Li L, Rose P, Tan C-H, Parkinson DB, and Moore PK. The effect of hydrogen sulfide donors on lipopolysaccharide-induced formation of inflammatory mediators in macrophages. *Antioxid Redox Signal* 12: 1147–1154, 2010.
53. Wrighting DM and Andrews NC. Interleukin-6 induces hepcidin expression through STAT3. *Blood* 108: 3204–3209, 2006.
54. Yuan Z-l, Guan Y-j, Chatterjee D, and Chin YE. Stat3 dimerization regulated by reversible acetylation of a single lysine residue. *Science* 307: 269–273, 2005.
55. Zanardo RC, Brancaleone V, Distrutti E, Fiorucci S, Cirino G, and Wallace JL. Hydrogen sulfide is an endogenous modulator of leukocyte-mediated inflammation. *FASEB J* 20: 2118–2120, 2006.
56. Zheng M, Qiao W, Cui J, Liu L, Liu H, Wang Z, and Yan C. Hydrogen sulfide delays nicotinamide-induced premature senescence via upregulation of SIRT1 in human umbilical vein endothelial cells. *Mol Cell Biochem* 393: 59–67, 2014.

Address correspondence to:
Prof. Yi Zhun Zhu
Shanghai Key Laboratory of Bioactive Small Molecules
Department of Pharmacology
School of Pharmacy
Fudan University
No. 826 Zhangheng Road
Pudong New Area
Shanghai 201203
China

E-mail: zhuyz@fudan.edu.cn; phczhuyz@nus.edu.sg

Date of first submission to ARS Central, February 28, 2015; date of final revised submission, June 18, 2015; date of acceptance, July 3, 2015.

Abbreviations Used

AOAA = aminooxyacetic acid
CBS = cystathionine β-synthase
CM = conditioned medium
CSE = cystathionine γ-lyase
DMEM = Dulbecco's modified Eagle's medium
GAPDH = glyceraldehyde-3-phosphate dehydrogenase
HDAC = histone deacetylase
IL-6 = interleukin-6
IP = immunoprecipitation
JAK2 = Janus kinase 2
LPS = lipopolysaccharide
PAG = propargylglycine
PBS = phosphate-buffered saline
PMA = phorbol myristate acetate
SIE = sis-inducible element
STAT3 = signal transducer and activator of transcription 3
SIRT1 = sirtuin 1
WT = wild-type